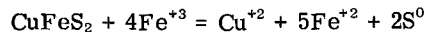


Reaction Mechanism for the Acid Ferric Sulfate Leaching of Chalcopyrite

P. B. MUNOZ, J. D. MILLER, AND M. E. WADSWORTH

The acid ferric sulfate leaching of chalcopyrite,

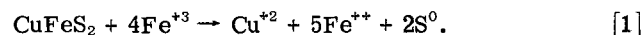


was studied using monosize particles in a well stirred reactor at ambient pressure and dilute solid phase concentration in order to obtain fundamental details of the reaction kinetics. The principal rate limiting step for this electrochemical reaction appears to be a transport process through the elemental sulfur reaction product. This conclusion has been reached in other investigations and is supported by data from this investigation in which the reaction rate was found to have an inverse second order dependence on the initial particle diameter. Furthermore, the reaction kinetics were found to be independent of Fe^{+3} , Fe^{+2} , Cu^{+2} and H_2SO_4 in the range of additions studied. The unique aspect of this particular research effort is that data analysis, using the Wagner theory of oxidation, suggests that the rate limiting process may be the transport of electrons through the elemental sulfur layer. Predicted reaction rates calculated from first principles using the physicochemical properties of the system (conductivity of elemental sulfur and the free energy change for the reaction) agree satisfactorily with experimentally determined rates. Further evidence which supports this analysis includes an experimental activation energy of 20 kcal/mol (83.7 kJ/mol) which is approximately the same as the apparent activation energy for the transfer of electrons through elemental sulfur, 23 kcal/mol (96.3 kJ/mol) calculated from both conductivity and electron mobility measurements reported in the literature.

HYDROMETALLURGICAL processes are playing an increasingly important role in the development of new technology for processing copper sulfide concentrates. Conventionally, these concentrates are processed by smelting and converting methods which, while achieving high recoveries of copper and precious metals, also produce large quantities of sulfur dioxide (SO_2) gas. Venting of this off-gas to the atmosphere represents a potential ecological hazard and has resulted in processing constraints on domestic copper producers in the form of costly pollution abatement equipment. These restrictions, in conjunction with the rising costs of fuel and the necessity to process low-grade ores that cannot be economically upgraded by conventional milling, concentration and smelting, have opened the door to the development of hydrometallurgical alternatives to compete with the traditional methods of copper production. Hydrometallurgy offers several possible alternative processes for producing copper from sulfide concentrates without producing SO_2 and frequently offers the possibility of direct recovery of most of the sulfur in the solid state. Roman and Benner¹ have summarized the leaching characteristics of many different copper sulfide systems. Dasher² discussed the economics of various hydrometallurgical processes and indicated that there are several routes to produce copper from sulfide concentrates that are potentially competitive with smelters. In the search

for hydrometallurgical alternatives to copper smelting, sulfuric acid, in conjunction with various oxidizing agents, has received more attention than any other reagent combination. Low cost, minimal corrosion problems, and the ability to regenerate sulfuric acid during electrowinning of copper are the main reasons for the interest in sulfuric acid systems.

In sulfuric acid solutions of ferric sulfate, chalcopyrite dissolves according to the following reaction,



This reaction stoichiometry has been observed by a number of investigators³⁻⁶ and has been confirmed in this study. Exceptions to this consensus are the early work of Sullivan⁷ and the more recent results reported by Jones and Peters.⁸ Sullivan found 22 pct sulfur oxidation to sulfate in 42 days and Jones and Peters reported 18 pct after approximately 17 days with even greater amount for shorter periods of time. Evidently the source of chalcopyrite, its pretreatment and the rate and extent of reaction may all influence the degree of sulfate formation.

The formation of an elemental sulfur layer on the chalcopyrite surface may significantly influence the reaction kinetics by establishing a diffusion barrier. The details of rate control for this particular reaction have not been well established. Some investigators^{3,8} attribute rate control to a *surface reaction*. Under certain circumstances, for example high anodic potentials, it appears that the elemental sulfur does not form a protective barrier and the reaction may be controlled by a *surface reaction*.⁹ Other investigators^{4-6,10,11} report that the reaction rate is limited by *transport in the chalcopyrite lattice or through the elemental sulfur reaction product layer*. When the ele-

P. B. MUNOZ, formerly Metallurgy Graduate Student, University of Utah, is now Visiting Professor, Organization of American States, Universidad Central de Venezuela, Caracas, Venezuela, and J. D. MILLER and M. E. WADSWORTH are Professors of Metallurgy and Metallurgical Engineering, University of Utah, Salt Lake City, UT 84112.

Manuscript submitted July 5, 1978.

Table I. Summary of Reaction Kinetics for Ferric Sulfate Leaching of Chalcopyrite

Investigators	System and Observations	Activation Energy, kcal/mol	Suggested Rate Limiting Process
Dutrillac, <i>et al</i> (1969)	Rotating disc technique. Natural (Temagami) and synthetic CuFeS ₂ . Rate independent of ferric concentration. Parabolic kinetics.	17.3 (50 to 99°C)	Transport control. Diffusion of ferrous ions through elemental sulfur.
Lowe (1970)	Continuous flow of solution through packed bed of particles (4 X 14 mesh). Rate independent of Fe ₂ (SO ₄) ₃ H ₂ SO ₄ concentrations.	17.8 (32 to 52°C)	Surface reaction controlled. Surface saturation followed by chemical reaction.
Baur, <i>et al</i> (1974)	Suspended particles (5 to 40 μ) in stirred reactor. Transvaal CuFeS ₂ . Parabolic kinetics.	20.3 (27 to 91.5°C)	Transport control. Diffusion of ferric ions through elemental sulfur.
Jones and Peters (1976)	Stirred reactor, 90°C, massive (≈ 1.0 cm cubes) and particulate (12 to 400 mesh) CuFeS ₂ from Craigmont Mine B.C. Some S ⁰ oxidized to SO ₄ . No particle size dependence below 48 mesh. Linear kinetics to 40 pct reacted.		Electrochemical surface reaction.
Beckstead, <i>et al</i> (1976)	Stirred reactor, monosize CuFe ₂ S particles and attritor ground particles prepared from Pima concentrate (1 to 40 μ). Rate independent of Fe ₂ (SO ₄) ₃ , FeSO ₄ , CuSO ₄ and H ₂ SO ₄ concentrations. Well defined rate dependence on particle size. Parabolic kinetics.	20.0 (60 to 90°C)	Transport control. Diffusion of ferric ions through elemental sulfur.

mental sulfur reaction product does appear to form a diffusion barrier and the rate becomes limited by transport through this layer, rather large activation energies have been observed. Baur *et al*, using radiochemical techniques, found diffusional rate control for Transvaal chalcopyrite after approximately 5.3×10^{-6} g cm⁻² chalcopyrite had reacted at 85°C. This corresponds to a thickness of consumed chalcopyrite of approximately 1.25×10^{-6} cm which is necessary to form the coherent diffusional-resistant layer of sulfur. Some question of this interpretation of rate control arises because of the large activation energies observed which normally are not observed for rate control by pore transport processes in other hydrometallurgical systems. In a previous publication⁶ these high activation energies had been explained to be due to a surface diffusion process and/or the idea that the porosity and tortuosity in the sulfur layer are highly temperature dependent and change in such a way to give an apparent activation energy of 20 kcal/mol. Another concern of the mass transport model is that the reaction kinetics are largely independent of both reactant (Fe⁺³) and product (Fe⁺², Cu⁺²) concentrations; results which are not consistent with the model. This anomalous situation has been explained as either being due to complexation reactions which maintain a constant reactant activity or due to adsorption and surface saturation of reactant.

The evaluation of the evidence supporting these positions has led to divergent views regarding the nature of the rate limiting step in the reaction sequence. The object of this investigation is to reexamine the rate data and analyze the results with a rather unique model more consistent with the experimental data. A summary of the results of investigations on the ferric sulfate leaching of chalcopyrite are presented in Table I.

EXPERIMENTAL

Experiments were designed to study the effects of various parameters on the reaction rate of monosize particles at low percent solids. The reaction kinetics

were followed by copper analysis of solution samples taken at timed intervals.

Materials

The chalcopyrite mineral used in this study was obtained from a Pima concentrate. Table II shows the chemical and mineralogical analysis of the concentrate in the condition it was received.

Monosize material was prepared from the concentrate by wet screening and sizing with a Warman Cyclosizer. During the sample preparation process, the particles were dispersed with an ultrasonic probe for 15 min to break-up agglomerates prior to the final screening. Previously, Beckstead and Miller¹² reported the importance of the sample preparation procedure. Two narrow size fractions, $63 \times 47 \mu$ and $16 \times 12 \mu$ were selected and characterized by their smallest size, 47 and 12 μ, respectively. These fractions were passed through a Carpc Laboratory Magnetic Separator, in order to remove quartz and pyrite impurities, upgrading the monosize sample to approximately 87 pct chalcopyrite. Also a $5 \times 2 \mu$ monosize sample was prepared from the concentrate by the Donaldson Company with an Accucut Model B air classifier. Microscopic analysis of this material indicated an average particle diameter of 4 μ, a value which was also confirmed by air permeametry measurements

Table II. Analysis of Pima Concentrate

Chemical Analysis		Mineralogical Analysis	
Element	Percent	Mineral	Percent
Cu	27.2	CuFeS ₂	80
Fe	29.2	FeS ₂	5
S	30.8	SiO ₂	5
Sb	0.60	Al ₂ O ₃	0.93
Zn	0.50	CaO	0.52
Mo	0.14	Talc and chlorites	8
Pb	0.07		
As	0.02		

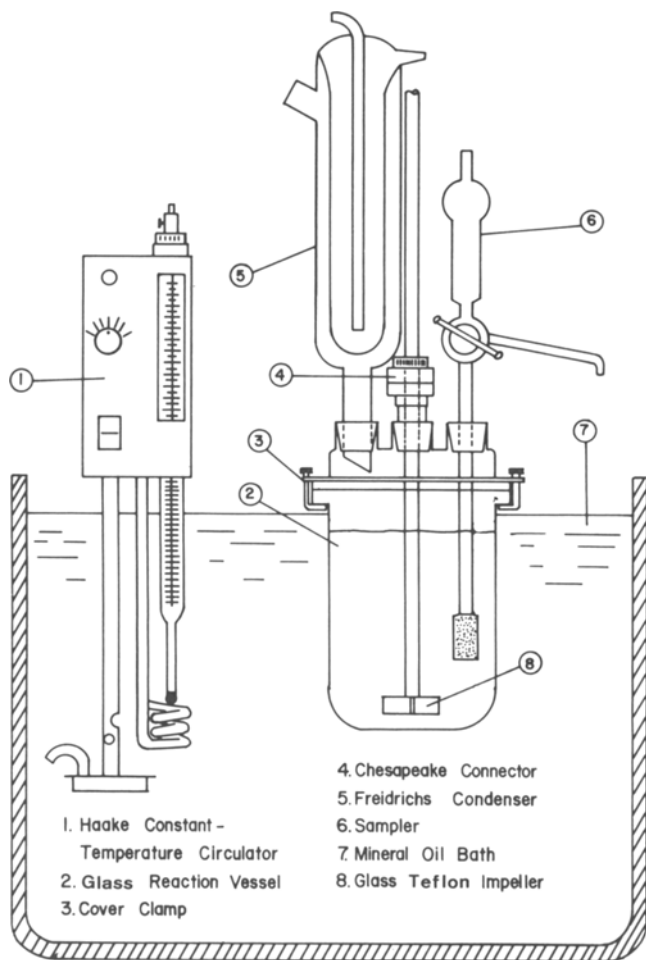


Fig. 1—Schematic diagram of leaching apparatus (about one-third scale).

with a Permaran apparatus. All monosize particles were examined with a microscope, with a Coulter-Counter, and with a Micromeritics Sedigraph in order to measure particle size. These measurements have given independent confirmation of the size assessment.¹³

Apparatus and Procedure

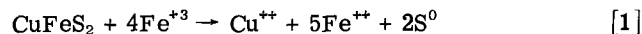
A schematic diagram of the experimental apparatus is given in Fig. 1. All leaching experiments were run in a one liter, baffled glass reaction kettle with clamp-held lids containing four fitted openings. A thermometer, solution sampler, Friedrich's condenser, and glass impeller were placed into the reactor through these openings. The turbine-type impeller was inserted through the center port by means of a Chesapeake stirrer connection. Perpendicular turbine blades were selected to impose maximum shear on the chalcopyrite particles and enhance mass transfer in the aqueous phase. The impeller was driven with a Fisher Dyna-Mix controller. The reactor was submerged in a circulating oil bath which was heated with a Haake temperature controller. Temperature was always held within ± 0.2 K.

Distilled water and reagent grade chemicals were used to prepare the desired leaching solutions. Samples of about 5 ml were taken through a fritted-glass sampling device at selected times and analyzed for

copper concentration with a Perkin-Elmer Model 305A atomic absorption spectrophotometer. Ferrous ion was analyzed by titration with a standard ceric sulfate solution using ferrion as an indicator.¹⁴

RESULTS AND DISCUSSION

The following stoichiometry was found for acid ferric sulfate leaching of chalcopyrite;



a result which agrees with that presented by Dutrizac.⁵ The topochemical nature of the leaching reaction is clearly illustrated in Fig. 2 which shows the cross section of a partially reacted chalcopyrite particle surrounded by a dense, tenacious sulfur layer. The reaction kinetics have been studied as a function of a number of variables including; particle size, temperature and concentration.

Particle Size Effect

The leaching response of 4, 12 and 47 μ monosize chalcopyrite particles is presented in Fig. 3, as fraction of copper reacted *vs* time plots for 1 M H_2SO_4 , 0.25 M $\text{Fe}_2(\text{SO}_4)_3$, 93°C, 0.5 pct solids and 1200 rpm. The rapid decrease in rate with time seems to be due to the formation of the sulfur layer on the surface of the chalcopyrite thus providing a diffusion barrier. The distinct reaction boundary between the outer sulfur product layer and the unreacted chalcopyrite core,

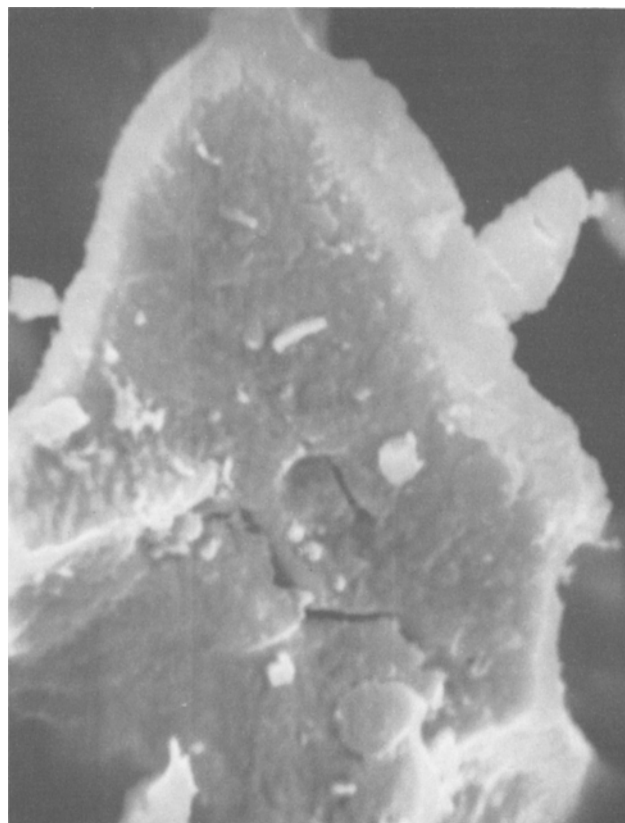


Fig. 2—A photomicrograph taken with a scanning electron microscope of the cross section of a partially leached chalcopyrite particle (10 μm) showing the sulfur layer and topochemical nature of the leaching response. (Magnification 3700 times).

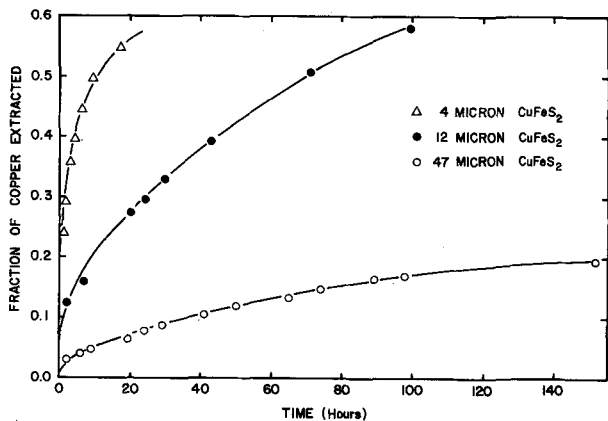


Fig. 3—A plot of fraction of copper extracted from monosize chalcopyrite particles as a function of time for 1.0 M H₂SO₄, 0.25 M Fe₂(SO₄)₃, 90°C, 0.5 pct solids and 1200 rpm.

as shown in Fig. 2, and the strong dependence of the rate of reaction on particle size, as shown in Fig. 3, suggests that a shrinking core-type model with rate control by transport through the reaction product layer might be appropriate to describe the acid ferric sulfate leaching of chalcopyrite. These results contrast with the results of Jones and Peters⁸ who report no particle size dependence of reaction kinetics below about 300 μ for Craigmont chalcopyrite.

For spherical particles, in which the reaction rate is controlled by transport through a reaction product layer, the following quasisteady state relationship between fraction reacted (α) and the time (t) is well established for a batch system.

$$F(\alpha) = 1 - (2/3)\alpha - (1 - \alpha)^{2/3} = k_p t \quad [2]$$

where k_p is the parabolic rate constant which involves many factors as will be discussed later and is inversely proportional to the square of the initial particle size.

According to Eq. [2] a plot of $F(\alpha)$ vs time should be linear with k_p as the slope. This plot is shown in Fig. 4 where, in fact, a linear relationship is observed. In addition, the parabolic rate constants (k_p) thus obtained should be inversely proportional to the square of the initial particle size. That is, a plot of k_p vs $(1/d_0^2)$ should also be linear. Figure 5 represents such a plot and the linear relationship further supports the

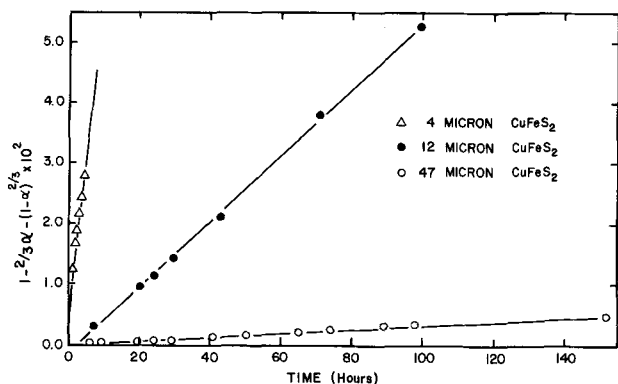


Fig. 4—A plot of the function, $1 - (2/3)a - (1 - a)^{2/3}$, for monosize chalcopyrite particles as a function of time for the data shown in Fig. 3.

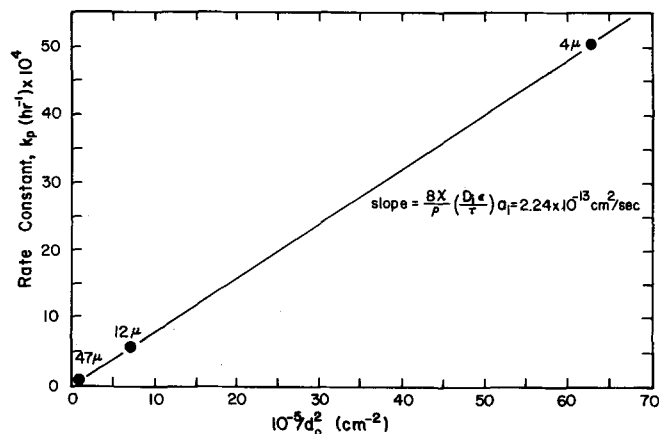


Fig. 5—A plot of the parabolic rate constant vs the square of the inverse initial particle diameter for the data shown in Fig. 4.

concept that the reaction rate is limited by a transport process through the reaction product layer.

Temperature Effect

Several tests were performed in order to determine the effect of temperature on the reaction kinetics. As the temperature was increased the reaction rate also increased as shown in Fig. 6 where the effect of temperature on the leaching response of 12 μ particles for 1 M H₂SO₄, 0.25 M Fe₂(SO₄)₃, 0.5 pct solids and 1200 rpm is presented. The temperature effect on the reaction kinetics of 4 μ particle size was also studied. In this case, low ionic strength conditions were used (0.01 M H₂SO₄, 0.03 M Fe₂(SO₄)₃, 0.3 pct solids and 1200 rpm). Figure 7 shows the leaching response of 4 μ particles for various temperatures.

The leaching responses of the 4 and 12 μ particles were linearized according to Eq. [2] from which the parabolic rate constants were obtained. These parabolic rate constants were normalized with respect to particle size and plotted on an Arrhenius plot. The Arrhenius equation for the temperature dependence of the normalized parabolic rate constant can be written as,

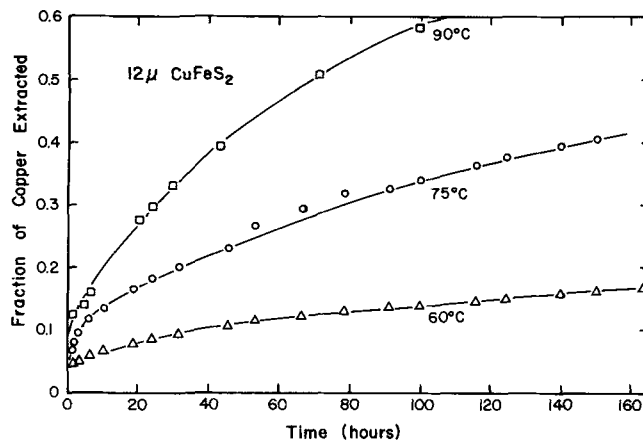


Fig. 6—A plot of fraction of copper extracted from 12 μ monosize chalcopyrite particles as a function temperature for 1.0 M H₂SO₄, 0.25 M Fe₂(SO₄)₃, 0.5 pct solids and 1200 rpm.

$$k_p \cdot d_0^2 = A \exp(-E_a/RT) \quad [3]$$

where

k_p = parabolic rate constant, (time⁻¹),
 A = frequency factor,
 R = universal gas constant, (calories/K),
 T = absolute temperature, (K),
 E_a = energy of activation, (calories), and
 d_0 = initial particle diameter, (cm).

Taking the logarithm of Eq. [3] the following expression is obtained:

$$\log(k_p \cdot d_0^2) = \log A - (E_a/2.303R)(1/T). \quad [4]$$

A plot of Eq. [4] is shown in Fig. 8 where a linear relationship is observed. This relationship holds for both 4 and 12 μ particles and, surprisingly, data for both sizes give approximately the same normalized parabolic rate constant, even though, the reactant concentration is different. This result is discussed below, under concentration effects. An activation energy, E_a , of 20 kcal/mol (83.7 kJ/mol) was calculated by regression analysis. The magnitude of E_a is high for a pore diffusion process and the significance of this result will be examined in the theory section.

Concentration Effect

Previous results⁶ had shown that the reaction kinetics were independent of Fe^{++} and Cu^{++} concentrations. Similarly the reaction kinetics were shown to be independent of H_2SO_4 concentration. The function of H_2SO_4 is simply to prevent hydrolysis of Fe^{+3} . Finally, it had been observed that the reaction kinetics were for the most part independent of the Fe^{+3} concentration.⁶ Only for low Fe^{+3} concentrations has a distinct dependence been observed.¹³

In general, as the concentration of Fe^{+3} is increased, an increase in the reaction rate would be expected especially if reactant transport were the rate limiting step. This effect was not observed in the acid ferric sulfate leaching of chalcopyrite. The ferric ion independence is revealed in the Arrhenius Plot (Fig. 8) in which the size normalized parabolic rate constants at 0.5 M Fe^{+3} for the 12 μ particles and at 0.06 M Fe^{+3} for the 4 μ particles are coincident. The linear rela-

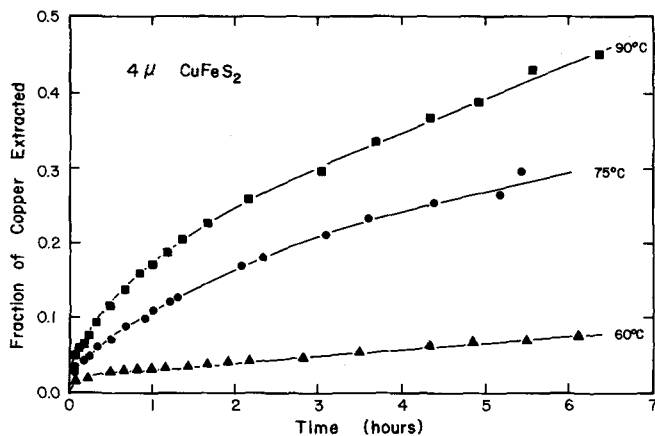


Fig. 7—A plot of fraction of copper extracted from 4 μ monosize chalcopyrite particles as a function of temperature for 0.01 M H_2SO_4 , 0.03 M $Fe_2(SO_4)_3$, 0.5 pct solids and 1200 rpm.

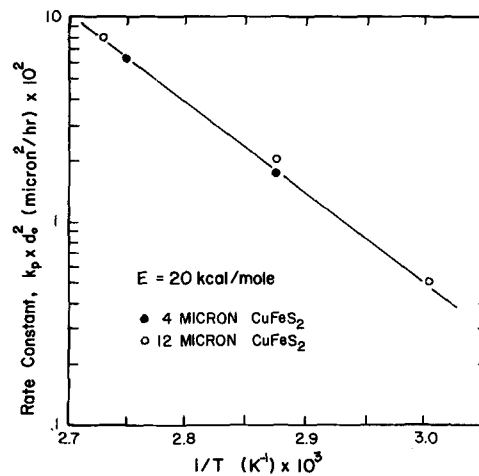


Fig. 8—Arrhenius plot for the ferric sulfate leaching of monosize chalcopyrite particles. The normalized parabolic rate constants $k_p d_0^2$, were determined from the data presented in Figs. 6 and 7.

tionship for different ferric ion concentrations indicates that the reaction kinetics are independent of the reactant concentration. The apparent zero order ferric ion dependence, also observed by other investigators,^{3,5,6,10} will be discussed later.

Initial Reaction Kinetics

From the results of this study it is seen that the overall reaction rate is limited predominantly by a transport process through the elemental sulfur product. However this process cannot be the rate limiting step during the initial stage of reaction since the sulfur layer is not present initially. Even though it appears that the initial stage of reaction offers little resistance with respect to the overall rate of reaction for the conditions of this study, it may be useful to summarize some of our results on initial reaction kinetics.¹³ These results may be particularly important under circumstances where the sulfur film is non-protective.

Initial reaction kinetics were studied by removing acid soluble copper before reaction initiation. Rate data from the initial stage of reaction was found to exhibit an inverse first order dependence on initial particle diameter, a half order dependence on ferric concentration and an activation energy of 8 kcal/mole (33.5 kJ/mol). The experimentally determined reaction velocity constant is approximately an order of magnitude less than that which would be expected if the rate were controlled by diffusion in the aqueous phase across a mass transfer boundary layer. On this basis it was concluded that the initial stage of reaction is controlled by an electrochemical reaction, the resistance of which does not contribute significantly to the resistance of the overall reaction kinetics.

Baur *et al*¹⁰ noted an initial surface reaction rate control for the dissolution of Transvaal chalcopyrite in the presence of oxygen. Jones and Peters⁸ clearly established the electrochemical character of the initial dissolution process for Craigmont chalcopyrite. The latter investigators measured the mixed potential during leaching which was found to vary linearly with $\log[Fe^{3+}]$. Introduction of the mixed potential into a Butler-Volmer expression for the dissolution process

Table III. Initial Rate of Reaction for Ferric Sulfate Leaching of Chalcopyrite

Investigator	Chalcopyrite Source	Ferric Concentration	Temperature	Initial Rate $\frac{g(\text{CuFeS}_2)}{\text{cm}^2 \text{ h}}$
Dutrizac <i>et al</i> ⁵	Synthetic	0.11 M	94°C	1.15×10^{-4}
Baur <i>et al</i> ¹⁰	Transvaal	0.4 M	85°C	1.97×10^{-4}
Jones and Peters ⁸	Craigmont	1.0 M	90°C	5.73×10^{-4}
Present Investigation	Pima	1.0 M	90°C	2.05×10^{-4}

results in an apparent half-power dependence on the ferric concentration as was observed in this study. Review of initial reaction rate data reported in the literature is compared together with that of the present investigation in Table III. Note that the initial rates are nearly the same for the Transvaal and Pima samples in which the reaction quickly becomes transport controlled whereas the initial rate is almost three times faster for the Craigmont sample in which the reaction does not appear to be limited by a transport process. Under these circumstances in which the electrochemical reaction limits the reaction kinetics, it seems that an intermediate defect structure forms at the surface accompanied by either incomplete sulfur coverage or a sulfur layer with high porosity.

THEORETICAL

From the analysis of reaction kinetics controlled by diffusion through a product layer, the following quasi-steady state shrinking core rate expression can be obtained, assuming spherical particles:

$$\frac{dn(\text{CuFeS}_2)}{dt} = \frac{(b/a)4\pi D\Delta C r r_0}{r_0 - r} \quad [5a]$$

or in terms of fraction reacted (α)

$$\frac{d\alpha}{dt} = \frac{3(b/a)DC(1-\alpha)^{1/3}}{\rho_B r_0^2 [1 - (1-\alpha)^{1/3}]} \quad [5b]$$

where,

α = fraction CuFeS_2 reacted at time t ,

b/a = stoichiometry factor, χ , moles CuFeS_2 reacted per mole of transported species,

D = effective diffusion coefficient ($D_i\epsilon/\tau$) for transport through product layer, where ϵ is the porosity and τ is the tortuosity,

ΔC = difference in concentration or activity (a_i) of transported species between the aqueous phase and the unreacted core,

t = time,

r = radius of unreacted core at time t ,

r_0, d_0 = initial particle size, radius and diameter respectively, and

ρ_B = molar density chalcopyrite.

For constant concentration of reactant and assuming the concentration of the transported reactant at the surface of the unreacted core is zero, Eq. [5b] can be integrated to yield the following relationship between fraction reacted and time for a batch leaching system.

$$1 - (2/3)\alpha - (1 - \alpha)^{2/3} = k_p t \quad [2]$$

where

$$k_p = \frac{8\chi}{\rho} \left(\frac{D_i\epsilon}{\tau} \right) a_i \frac{1}{d_0^2} \text{ (time}^{-1}\text{)}.$$

It is apparent that a plot of k_p vs $(1/d_0^2)$ should be linear with $(8\chi/\rho)(D_i\epsilon/\tau)a_i$ as the slope. Such a plot is shown in Fig. 5, from which a slope of 2.24×10^{-13} (cm^2/s) was calculated by regression analysis. On first examination, this analysis of the experimental data with respect to initial particle diameter seems to explain the observed rate behavior. Assuming control by the transport of ferric ion, the value of an effective diffusion coefficient ($D_{\text{Fe}}\epsilon/\tau$) for the ferric ion can be estimated to be $\sim 10^{-13}$ cm^2/s . Even if extreme values for the porosity and tortuosity are selected, it is difficult to justify such a small value for the effective diffusion coefficient in terms of a pore diffusion model. Furthermore, as is seen from the integrated diffusion equation, Eq. [2], the proportionality constant, k_p , should have a first order dependence on the concentration or activity of the ferric ion. Such appears not to be the case as shown by data presented in Fig. 8 and data reported in the literature.^{3,5,6,10} Although due to complexation reactions the rate dependence on ferric addition should be diminished, it is difficult to justify complete independence on this basis as previously suggested.⁶ For example, for a thirty-fold increase in $\text{Fe}_2(\text{SO}_4)_3$, the ferric activity increases by a factor of 6. Under these circumstances the rate would not be expected to be directly proportional to the $\text{Fe}_2(\text{SO}_4)_3$ addition, but at least the rate should have increased by a factor of 6 which it did not. Finally, the observed activation energy of 20 kcal/mol (83.7 kJ/mol) is much larger than normally would be expected for a pore diffusion process. In view of this analysis, further consideration of the rate process must be given to explain the anomalous behavior. Species other than ferric ion which are transported through the sulfur layer and which might limit the reaction rate include, ferrous ions, cupric ions, and, in particular, electrons.

Wagner Theory

In describing the transport of ions and electrons through the sulfur reaction product both the diffusion due to chemical potential, μ , and that due to the electrical potential, ϕ , must be taken into account. In this context, the flux, in moles of species passing per unit time through a cross section of 1 cm^2 for anions, cations, electrons, or in general the i -th species, can be represented by¹⁵

$$J_i = - \frac{t_i \sigma}{Z_i^2 e^2} \left(\frac{d\mu_i}{dx} + Z_i e \frac{d\phi}{dx} \right) \quad [6]$$

where

$d\mu_i/dx$ = chemical potential gradient,

$d\phi/dx$ = electric field strength,

e = electronic charge,

t_i = transport number,

σ = electrical conductivity, and

Z_i = valence of species i .

Equation [6] is the general expression for the flux of species i and will be applied to the ferric sulfate leaching of chalcopyrite.

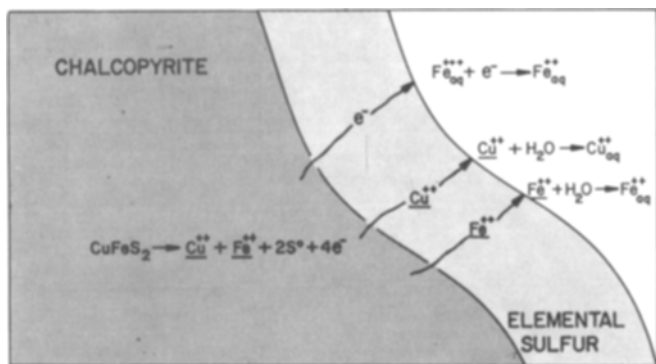


Fig. 9—Schematic representation of the transport process in the ferric sulfate leaching of chalcopyrite. Note that the hydrated ferric ion does not advance through the sulfur product layer, but rather is discharged at the sulfur-solution interface.

Leaching Model

The ferric sulfate leaching of chalcopyrite is considered in terms of the Wagner Theory and the transport processes are depicted in Fig. 9. The potential difference across the sulfur product layer develops due to the separation of the anodic and cathodic half cells. In order to eliminate $d\phi/dx$ from Eq. [6] use is made of the fact that no net current flows through the sulfur layer during the stationary state. In other words, electroneutrality requires that;

$$2J_{\text{Cu(II)}} + 2J_{\text{Fe(II)}} + 3J_{\text{Fe(III)}} = J_e \quad [7]$$

Assuming that transport of the hydrated Fe^{+3} toward the inner boundary is negligible and also that,

$$J_{\text{Cu(II)}} = J_{\text{Fe(II)}} \quad (\text{coupled mass transfer}) \quad [8]$$

then, Eq. [7] becomes

$$2J_{\text{Cu(II)}} + 2J_{\text{Fe(II)}} = J_e = 4J_{\text{Fe(II)}} \quad [9]$$

From Eq. [6], expressions for $J_{\text{Fe(II)}}$, $J_{\text{Cu(II)}}$, and J_e can be obtained:

$$J_{\text{Fe(II)}} = -\frac{t_{\text{Fe(II)}}\sigma}{4e^2} \left(\frac{d\mu_{\text{Fe(II)}}}{dx} + 2e \frac{d\phi}{dx} \right) \quad [10]$$

$$J_{\text{Cu(II)}} = -\frac{t_{\text{Cu(II)}}\sigma}{4e^2} \left(\frac{d\mu_{\text{Cu(II)}}}{dx} + 2e \frac{d\phi}{dx} \right) \quad [11]$$

and

$$J_e = -\frac{t_e\sigma}{e^2} \left[\frac{d\mu_e}{dx} - e \frac{d\phi}{dx} \right] \quad [12]$$

Substituting Eqs. [10], [11], and [12] into Eq. [9] results in:

$$\begin{aligned} \frac{t_{\text{Fe(II)}}\sigma}{2e^2} \left(\frac{d\mu_{\text{Fe(II)}}}{dx} + 2e \frac{d\phi}{dx} \right) + \frac{t_{\text{Cu(II)}}\sigma}{2e^2} \left(\frac{d\mu_{\text{Cu(II)}}}{dx} + 2e \frac{d\phi}{dx} \right) \\ = \frac{t_e\sigma}{e^2} \left(\frac{d\mu_e}{dx} - e \frac{d\phi}{dx} \right) \end{aligned} \quad [13]$$

Rearranging the expression;

$$(t_{\text{Fe(II)}} + t_{\text{Cu(II)}} + t_e) e \frac{d\phi}{dx} = t_e \frac{d\mu_e}{dx} - \frac{t_{\text{Fe(II)}}}{2} \frac{d\mu_{\text{Fe(II)}}}{dx}$$

$$- \frac{t_{\text{Cu(II)}}}{2} \frac{d\mu_{\text{Cu(II)}}}{dx} \quad [14]$$

An expression for $d\mu_{\text{Cu(II)}}/dx$ can be obtained from the coupled mass transfer solution of Eq. [8], as follows;

$$\begin{aligned} t_{\text{Fe(II)}} \frac{d\mu_{\text{Fe(II)}}}{dx} + 2t_{\text{Fe(II)}} e \frac{d\phi}{dx} = t_{\text{Cu(II)}} \frac{d\mu_{\text{Cu(II)}}}{dx} \\ + 2t_{\text{Cu(II)}} e \frac{d\phi}{dx} \end{aligned} \quad [15]$$

Therefore;

$$\frac{d\mu_{\text{Cu(II)}}}{dx} = \frac{t_{\text{Fe(II)}}}{t_{\text{Cu(II)}}} \frac{d\mu_{\text{Fe(II)}}}{dx} + 2e \left[\frac{t_{\text{Fe(II)}}}{t_{\text{Cu(II)}}} - 1 \right] \frac{d\phi}{dx} \quad [16]$$

Substituting for $d\mu_{\text{Cu(II)}}/dx$, and recognizing that the sum of the transport numbers, $t_{\text{Cu(II)}} + t_{\text{Fe(II)}} + t_e = 1$, then Eq. [14] becomes;

$$\begin{aligned} e \frac{d\phi}{dx} = t_e \frac{d\mu_e}{dx} - \frac{t_{\text{Fe(II)}}}{2} \frac{d\mu_{\text{Fe(II)}}}{dx} - \frac{t_{\text{Fe(II)}}}{2} \frac{d\mu_{\text{Fe(II)}}}{dx} \\ - e(t_{\text{Fe(II)}} - t_{\text{Cu(II)}}) \frac{d\phi}{dx} \end{aligned} \quad [17]$$

Solving for the voltage gradient and recognizing that $1 - t_{\text{Cu(II)}} = t_{\text{Fe(II)}} + t_e$ then;

$$\begin{aligned} (1 + t_{\text{Fe(II)}} - t_{\text{Cu(II)}}) e \frac{d\phi}{dx} = (2t_{\text{Fe(II)}} + t_e) e \frac{d\phi}{dx} \\ = t_e \frac{d\mu_e}{dx} - t_{\text{Fe(II)}} \frac{d\mu_{\text{Fe(II)}}}{dx} \end{aligned} \quad [18]$$

Therefore

$$\frac{d\phi}{dx} = \frac{1}{e} \left(\left(\frac{t_e}{2t_{\text{Fe(II)}} + t_e} \right) \frac{d\mu_e}{dx} - \left(\frac{t_{\text{Fe(II)}}}{2t_{\text{Fe(II)}} + t_e} \right) \frac{d\mu_{\text{Fe(II)}}}{dx} \right) \quad [19]$$

Substitution of $(d\phi/dx)$ in Eq. [10] results in

$$\begin{aligned} J_{\text{Fe(II)}} = -\frac{t_{\text{Fe(II)}}\sigma}{4e^2} \left(\frac{d\mu_{\text{Fe(II)}}}{dx} + \left(\frac{2t_e}{2t_{\text{Fe(II)}} + t_e} \right) \frac{d\mu_e}{dx} \right. \\ \left. - \left(\frac{2t_{\text{Fe(II)}}}{2t_{\text{Fe(II)}} + t_e} \right) \frac{d\mu_{\text{Fe(II)}}}{dx} \right) \end{aligned} \quad [20]$$

If transport of electrons across the sulfur layer is considered to be the rate controlling step, then the transport number for electrons, is much smaller than the transport number for Fe^{+2} ,

$$t_e \ll t_{\text{Fe(II)}} \quad [21]$$

Under these conditions Eq. [20] becomes;

$$J_{\text{Fe(II)}} = -\frac{t_e\sigma}{2e^2} \frac{d\mu_e}{dx} \quad [22]$$

Since,

$$J_{\text{Fe(II)}} = \frac{1}{A} \frac{dn}{dt} (\text{CuFeS}_2) \quad [23]$$

where A is the area of the unreacted core, then Eq. [22], for spherical coordinates, becomes

$$\frac{dn}{dt} (\text{CuFeS}_2) = -(4\pi r^2) \frac{t_e \sigma}{4e^2} \frac{d\mu_e}{dr} \quad [24]$$

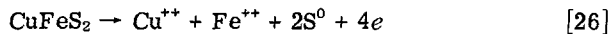
Assuming quasisteady state, integration of Eq. [24] for all values of r between r and r_0 , results in the following expression:

$$\frac{dn}{dt} (\text{CuFeS}_2) = -\frac{4\pi r r_0}{(r_0 - r)} \left(\frac{t_e \sigma}{4e^2}\right) (\mu_e^o - \mu_e^i) \quad [25]$$

where μ_e^o and μ_e^i are the chemical potentials for electrons at the outer and inner phase boundary respectively.

The ferric sulfate leaching of CuFeS_2 may be viewed as two half cell reactions which occur on opposite sides of the sulfur layer as shown in Fig. 9.

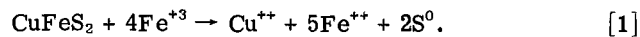
Inner boundary:



Outer boundary:



The overall reaction, including the hydration of the transported Cu^{++} and Fe^{++} ions, is;



Therefore

$$\Delta G = 2\mu_{\text{S}^0} + 5\mu_{\text{Fe(II)}} + \mu_{\text{Cu(II)}} - (4\mu_{\text{Fe(III)}} + \mu_{\text{CuFeS}_2}) \quad [28]$$

Now, from Eqs. [26] and [27], the following expressions are obtained:

$$\mu_{\text{CuFeS}_2} = \mu_{\text{Cu(II)}} + \mu_{\text{Fe(II)}} + 2\mu_{\text{S}^0} + 4\mu_e^i \quad [29]$$

and

$$4\mu_{\text{Fe(III)}} + 4\mu_e^o = 4\mu_{\text{Fe(II)}} \quad [30]$$

Combining Eqs. [29] and [30] results in

$$\begin{aligned} (\mu_e^o - \mu_e^i) &= 4\mu_{\text{Fe(II)}} - \mu_{\text{CuFeS}_2} + \mu_{\text{Cu(II)}} + \mu_{\text{Fe(II)}} \\ &+ 2\mu_{\text{S}^0} - 4\mu_{\text{Fe(III)}} = 2\mu_{\text{S}^0} + 5\mu_{\text{Fe(II)}} \\ &+ \mu_{\text{Cu(II)}} - 4\mu_{\text{Fe(III)}} - \mu_{\text{CuFeS}_2} \end{aligned}$$

and it is recognized from Eq. [28] that,

$$(\mu_e^o - \mu_e^i) = \Delta G \quad [31]$$

which can be substituted in Eq. [25] resulting in

$$\frac{dn}{dt} (\text{CuFeS}_2) = -\frac{4\pi r r_0}{(r_0 - r)} \left(\frac{t_e \sigma}{4e^2}\right) \Delta G \quad [32]$$

Equation [32] can then be equated to Eq. [5a] resulting in

$$\frac{D\Delta C}{4} = \frac{t_e \sigma}{4e^2} \Delta G \quad [33]$$

where

$t_e \sigma$ = electrical conductivity of the sulfur layer (ohm⁻¹ cm⁻¹),

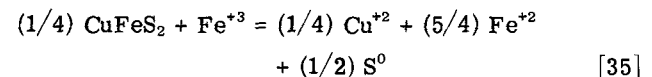
ΔG = free energy of reaction, and

e = electronic charge, 96,500 (Coulombs/equiv.) or 23,060 (cal/equiv · volt).

Combining Eq. [5b] and Eq. [33], a general expression for the rate in terms of fraction reacted, α , and the physicochemical properties of the system (conductivity of elemental sulfur and the free energy of reaction) is obtained;

$$\frac{d\alpha}{dt} = (300) \frac{3t_e \sigma \Delta G}{\rho_B d_0^2 e^2} \frac{(1 - \alpha)^{1/3}}{[1 - (1 - \alpha)^{1/3}]} \quad [34]$$

where the value 300 converts volts from electrostatic units (esu) to practical volts. For the reaction under consideration,



a value of -9310 calories for the standard free energy of reaction at 363 K was obtained from;

$$\begin{aligned} \Delta G_R^0 (363 \text{ K}) &= \Delta H_R^0 (298 \text{ K}) - T \Delta S_R^0 (298 \text{ K}) \\ &= -9310 \text{ calories} \end{aligned} \quad [36]$$

assuming negligible changes in heat capacity over the temperature range in question and using the thermodynamic properties of the system listed in Table IV. The free energy expression is,

$$\Delta G = \Delta G_R^0 + RF \ln \frac{(a_{\text{Fe(II)}})^{5/4} (a_{\text{Cu(II)}})^{1/4}}{(a_{\text{Fe(III)}})} \quad [37]$$

or in terms of the fraction of copper extracted (α), and the stoichiometry factor (χ), Eq. [37] becomes;

$$\begin{aligned} \Delta G &= -9520 + 1660 \log \{ C_B^{1/2} \cdot [\alpha^{3/2} / (\chi - \alpha)] \chi^{-1/2} \\ &\times [\gamma_{\text{Fe(II)}}^{5/4} \gamma_{\text{Cu(II)}}^{1/4} / \gamma_{\text{Fe(III)}}] \} \end{aligned} \quad [38]$$

where C_B is the initial ferric concentration in moles/liter, and γ_i is the activity coefficient of species i .

By substituting Eq. [38] into Eq. [34], the leaching response of 4 and 12 μ chalcopyrite particles, for initial ferric ion concentrations of 0.06 M and 0.5 M, respectively, at 90°C, can be evaluated providing the electrical conductivity for the elemental sulfur reaction product, $t_e \sigma$, is known. Using the electrical conductivity of sulfur as an adjustable parameter, the rate expression (Eq. [34]), including the ΔG function (Eq. [38]), was numerically integrated using the Adams-Moulton algorithm and fitted to the leaching response of the 4 μ chalcopyrite (data previously presented in Fig. 7). The fit of this mathematical expression is presented in Fig. 10 for $t_e \sigma = 7.6 \times 10^{-13}$ (ohm⁻¹ cm⁻¹). This value for the electrical conductivity of the ele-

Table IV. Thermodynamic Properties for the Acid Ferric Sulfate Chalcopyrite-System^{16, 17}

	ΔG_f^0 (298 K) (Kcal/mol)	ΔH_f^0 (298 K) (Kcal/mol)	S^0 (298 K) (Kcal/mol deg)
CuFeS ₂	-45.5	-45.5	29.87
Fe ⁺³	-2.52	-11.4	-70.1
Cu ⁺²	15.53	15.39	-23.6
Fe ⁺²	-20.30	-21.0	-27.0
S	0	0	7.62

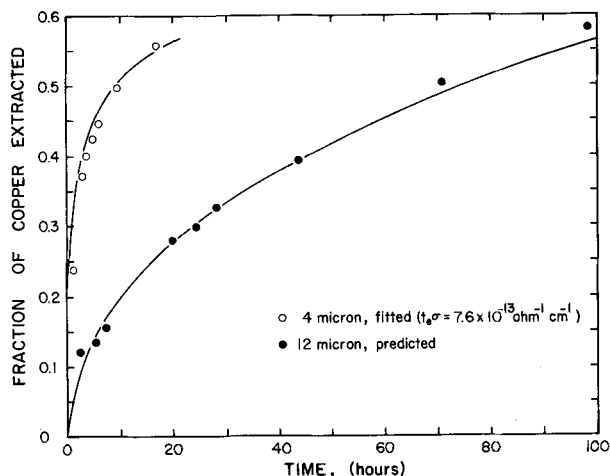


Fig. 10—Leaching response of both 4 and 12 μ monosize chalcopyrite particles at 90°C (other experimental conditions specified in Figs. 6 and 7). Data for the 4 μ response was fitted using the electrical conductivity of elemental sulfur as the only adjustable parameter. With this value, the leaching response of the 12 μ material was predicted.

mental sulfur reaction product can be compared with the value of 10^{-13} ($\text{ohm}^{-1} \text{cm}^{-1}$) for pure crystalline orthorhombic sulfur, at 90°C, as reported in the literature.¹³ The difference between the two values undoubtedly represents the impurities and polycrystalline nature of the elemental sulfur reaction product. It is known that minor impurity levels can cause increases in conductivity of up to two orders of magnitude greater than that for pure crystalline sulfur.

The leaching response of 12 μ chalcopyrite (data previously presented in Fig. 3) can now be predicted by using the electrical conductivity determined from the fit of the 4 μ data. The results of this computation are presented in Fig. 10 and as can be seen, the predicted response compares favorably with the experimental data. It is important to note that this prediction not only involved consideration of a change in particle size but also a change in ferric sulfate concentration by almost one order of magnitude. As can be seen from Eq. [38], the free energy change will not be very sensitive to the initial ferric concentration due to the logarithmic dependence and as a result, the reaction rate will appear to exhibit essentially zero order dependence on the ferric ion concentration. The results obtained by considering the variation of ΔG with the extent of the reaction seem to confirm the concept that the transport of electrons through the elemental sulfur layer is the rate controlling step.

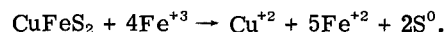
Further support for this reaction mechanism is given by the temperature dependence of the electrical conductivity of sulfur. From the electrical conductivity data presented in Table V, an apparent activation

energy for electronic transport can be calculated and is found to be 23 kcal/mole by regression analysis. This value of the activation energy for electronic transport, is very close to the experimental activation energy, 20 kcal/mol (83.7 kJ/mol), for ferric sulfate leaching of chalcopyrite (see Fig. 8). In addition, electron hopping transport and trapping phenomena in sulfur crystals have been studied by several investigators.^{19,20} A value of 1 ev, 23 kcal/mol (96.3 kJ/mol), for the trapping mechanism has been reported which agrees very well with the value calculated from the conductivity data presented in Table V.

The above information and data analysis seems to confirm that transport of electrons through the sulfur layer is indeed a possible explanation for the reaction kinetics observed in the acid ferric sulfate leaching of chalcopyrite.

CONCLUSIONS

The electrochemical reaction of chalcopyrite with sulfuric acid solutions of ferric sulfate conforms to the following reaction stoichiometry:



The chief function of the acid appears to be to prevent the hydrolysis of ferric ion. The experimental rate data and a theoretical analysis using the Wagner theory of oxidation, strongly suggests that the rate limiting step is the transport of electrons through the elemental sulfur layer. This conclusion is supported by the following results and analysis:

- 1) The rate of reaction was independent of the ferric ion concentration.
- 2) The rate of reaction was found to be dependent on the inverse square of the initial particle diameter.
- 3) The rate of reaction was independent of the initial ferrous and cupric concentrations. In other words, back reaction kinetics were not important in the reaction.
- 4) The rate of reaction was significantly dependent on temperature. The value of 20 kcal/mol (83.7 kJ/mol) for the activation energy, was shown to be approximately the same as the activation energy for transport of electrons through elemental sulfur, 23 kcal/mol (96.3 kJ/mol), calculated from conductivity measurements reported in the literature.¹⁸
- 5) The following theoretical rate expression describes electronic transport through the reaction product layer:

$$\frac{d\alpha}{dt} = 300 \frac{3t_e \sigma \Delta G}{\rho_b d_0^2 e^2} \cdot \frac{(1 - \alpha)^{1/3}}{[1 - (1 - \alpha)^{1/3}]}$$

From this expression and in conjunction with the ΔG function (Eq. [38]), the electrical conductivity of the elemental sulfur, $t_e \sigma$, was estimated from the leaching response of 4 μ particles by numerical integration. The fitted value for the electrical conductivity of the elemental sulfur reaction product, $t_e \sigma = 7.6 \times 10^{-13}$ ($\text{ohm}^{-1} \text{cm}^{-1}$), compares favorably with the electrical conductivity of pure crystalline orthorhombic sulfur at 90°C, $t_e \sigma = 10^{-13}$ ($\text{ohm}^{-1} \text{cm}^{-1}$), reported in the literature.¹⁸ Such agreement is quite satisfactory since it is known that minor impurity levels can cause increases in electrical conductivity of up to two orders

Table V. Electrical Conductivity of Elemental Sulfur¹⁸

Temperature, K	Electrical Conductivity ($\text{ohms}^{-1} \text{cm}^{-1}$)
293	5.24×10^{-18}
303	2.56×10^{-17}
342	2.54×10^{-16}
385	1.35×10^{-13}

of magnitude greater than that for pure sulfur. Importantly, it was shown that the leaching response of 12 μ chalcopyrite could be predicted using the fitted value for the electrical conductivity of the elemental sulfur reaction product obtained from the 4 μ leaching data, even though the particle size and initial ferric concentration differed significantly.

ACKNOWLEDGMENTS

This research project was financed by the RANN Division of the National Science Foundation under Grant Number GI 40538. Assistance of the Salt Lake City Metallurgy Research Center of the U.S. Bureau of Mines is gratefully acknowledged.

REFERENCES

1. R. J. Roman, and B. R. Benner: *Minerals Sci. Eng.*, 1973, vol. 5, no. 1, pp. 3-24.
2. J. Dasher: *CIM Trans.*, 1973, vol. 76, pp. 80-88.
3. D. F. Lowe: Ph.D. thesis, University of Arizona, Tucson, Ariz., 1970.
4. H. G. Linge: *Hydrometallurgy*, 1976, vol. 2, pp. 51-64. See also H. G. Linge: *Hydrometallurgy*, 1976, vol. 2, pp. 219-33.
5. J. E. Dutrizac, R. J. C. MacDonald and T. R. Ingraham: *Trans. TMS-AIME*, 1969, vol. 245, pp. 955-59.
6. L. W. Beckstead, P. B. Munoz, J. D. Miller, J. A. Herbst, F. A. Olson, and M. E. Wadsworth: *Extractive Metallurgy of Copper II*, pp. 611-32, The Metallurgical Society of AIME, New York, 1976.
7. J. D. Sullivan: *Trans. AIME*, 1933, vol. 106, pp. 515-46.
8. L. W. Jones, and E. Peters: *Extractive Metallurgy of Copper II*, pp. 633-53, The Metallurgical Society of AIME, 1976.
9. G. W. Warren: Ph.D. thesis, Department of Metallurgy and Metallurgical Engineering, University of Utah, Salt Lake City, U., 1978.
10. J. P. Baur, H. L. Gibbs, and M. E. Wadsworth: USBM RI 7823, 1974.
11. E. Peters: *AIME Internat. Symp. on Hydromet.*, pp. 205-28, AIME, N.Y., 1973.
12. L. W. Beckstead and J. D. Miller: *Met. Trans. B*, 1977, vol. 8B, pp. 19-38.
13. P. B. Munoz: Ph.D. thesis, Department of Mining, Metallurgical and Fuels Engineering, University of Utah, Salt Lake City, U., 1977.
14. W. C. Pierce: *Quantitative Analysis*, pp. 312-15, John Wiley and Sons, New York, 1958.
15. P. Kofstad: *High Temperature Oxidation of Metals*, John Wiley and Sons, New York, 1966.
16. E. Peters: "Hydrometallurgy: Theory and Practice," *First Tutorial Symposium on Hydrometallurgy*, AIME, Denver, Co., 1972.
17. R. Garrels and C. Christ: *Solutions Minerals and Equilibria*, Freeman, Cooper Company, San Francisco, 1965.
18. W. N. Tuller: *The Sulfur Data Book*, p. 59, McGraw-Hill Book Company, Inc., 1954.
19. A. R. Adams and W. E. Spear: *J. Phys. Chem. Solids*, 1964, vol. 25, pp. 1113-18.
20. D. J. Gibbons and W. E. Spear: *J. Phys. Chem. Solids*, 1966, vol. 27, pp. 1917-25.